NANO LETTERS

pubs.acs.org/NanoLett

Letter

Folding a Single-Molecule Junction

Chuanli Wu,[⊥] Demetris Bates,[⊥] Sara Sangtarash,[⊥] Nicoló Ferri, Aidan Thomas, Simon J. Higgins, Craig M. Robertson, Richard J. Nichols, Hatef Sadeghi,* and Andrea Vezzoli*

Cite This: *Nano Lett.* 2020, 20, 7980−7986

Read Online

ACCESS | Metrics & More | Article Recommendations | Supporting Information

ABSTRACT: Stimuli-responsive molecular junctions, where the conductance can be altered by an external perturbation, are an important class of nanoelectronic devices. These have recently attracted interest as large effects can be introduced through exploitation of quantum phenomena. We show here that significant changes in conductance can be attained as a molecule is repeatedly compressed and relaxed, resulting in molecular folding along a flexible fragment and cycling between an anti and a syn conformation. Power spectral density analysis and DFT transport calculations show that through-space tunneling between two phenyl fragments is responsible for the conductance increase as the molecule is mechanically folded to the syn conformation. This phenomenon represents a novel class of mechanoresistive molecular devices, where the functional moiety is embedded in the conductive backbone and exploits intramolecular nonbonding interactions, in contrast to most studies where mechanoresistivity arises from changes in the molecule−electrode interface.

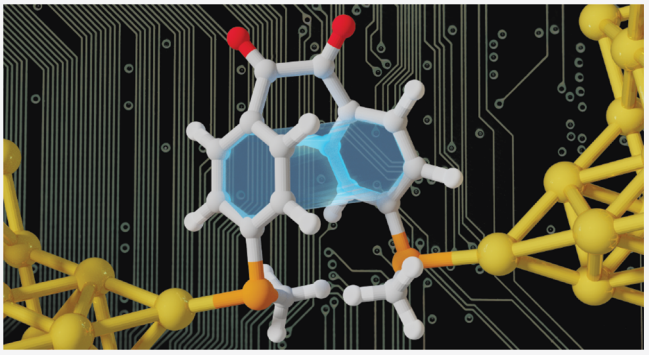

KEYWORDS: *single-molecule junctions, mechanoresistivity, conformational, switching, dionemolecular devices*

Apart from fundamental studies focusing on archetypal saturated compounds such as α,ω-alkanedithiols[1−3] and α,ω-alkanediamines,[4−6] the majority of molecular wires employed to fabricate molecular junctions are rodlike, π-conjugated structures. They have found such a widespread use because their extensive conjugation results in high conductance, and the conformationally rigid π-system avoids complications which could arise, for instance, from gauche defects in saturated carbon chains.[7,8] Controlled conformational flexibility, however, can be used to impart functionality. Franco et al. proposed a theoretical exploitation of flexible fragments in single-molecule junctions to develop force-sensitive single-molecule devices,[9] based on π-stacking perylene units linked by a saturated propyl chain, that would "unstack" as the junction is stretched. Stacks of phenyl rings and other simple heteroaromatics are able to act as efficient conductors in molecular junctions,[10,11] with charge transported through $\pi-\pi$ interactions.[12−18] In the device proposed by Franco et al., these effects are incorporated into a single molecule, where conductance is predicted to drop by orders of magnitude as the stacking configuration is mechanically unfolded and charge is forced to flow through the saturated propyl chain. Such a device would represent a new class of molecular electronic components responsive to mechanical stimuli, complementing the existing range that exploits changes in the electrode-molecule interface,[19−26] stereoelectronic configuration switching,[27,28] and stretching-dependent quantum interference effects[12,29] as the molecular junction is compressed and relaxed.

Intrigued by these phenomena, we designed molecule **1** to have two phenyl rings spaced by a diketone chain. The molecule has a conformationally flexible bond between the two sp^2-hybridized carbonyls (orange in Figure 1a). Although the ground state structure is a quasi-anti conformation, similar to benzil (an analogue of **1** without the thiomethyl termini),[30] the central C—C bond in such compounds has a dihedral torsional barrier of only 15−45 kJ/mol (0.15−0.5 eV) for interconversion between the syn and anti conformations.[31,32] We performed simple molecular mechanics calculations (MM2 Force Field) on **1** to obtain the ground state energy as a function of the (C═O)—(C═O) dihedral angle θ. We found that the energy profile has two minima with approximately 130° of difference between them (Figure 1) and shallow energy barriers. Our results suggest that a syn ($\theta < 90°$) ⇌ anti ($\theta > 90°$) conversion should be readily attained by compressing a metal−molecule−metal junction made with **1** and mechanically folding the molecule along the central C—C

Received: July 7, 2020
Revised: October 7, 2020
Published: October 13, 2020

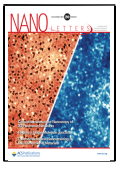

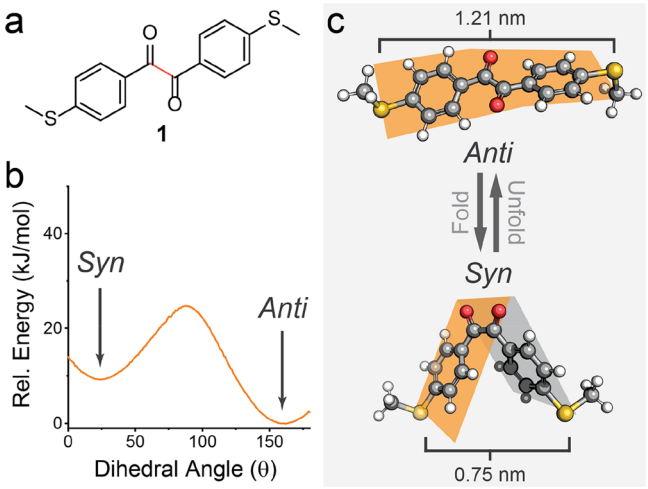

Figure 1. Molecular Design. (a) Structure of compound **1** with the conformationally flexible bond highlighted in orange. (b) Energy vs O═C—C═O dihedral angle for compound **1** obtained by MM2 Force Field calculations. (c) Three-dimensional structures of **1** in the anti (dihedral of 155°) and syn (dihedral of 23°) conformations with S−S length shown.

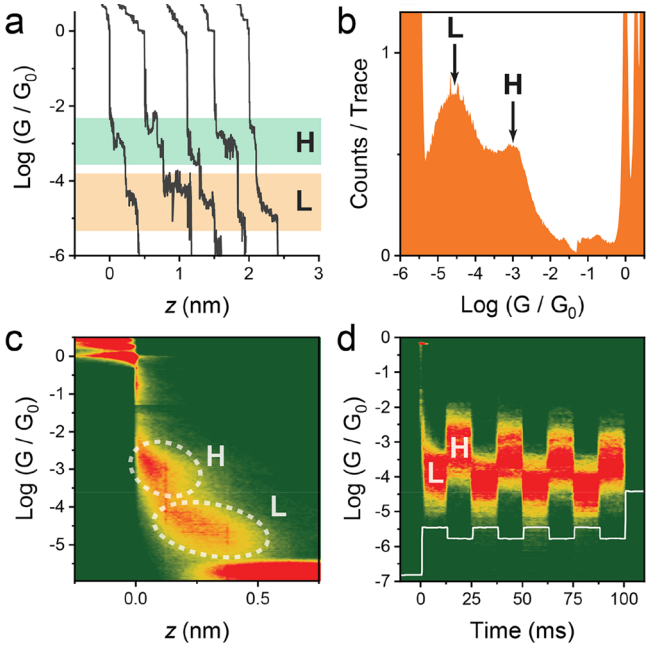

Figure 2. STM-BJ data for **1**. (a) Example G_z traces for **1** under constant electrode displacement speed (20 nm/s). (b) Conductance histogram for **1** compiled with 7678 traces as shown in (a) with no data selection. (c) Conductance−electrode displacement density map of **1**. (d) Density map of piezo-modulation experiments. After an abrupt 1.2 nm stretch that opens the nanogap, the junction size is compressed by 0.4 nm and then relaxed again for four times in 100 ms. The piezo signal is superimposed as a gray line for clarity. Histograms and 2D maps compiled with 100 bins/decade, 100 bins/nm, and 1000 bins/second. Experiments performed at 200 mV bias. White contours in (c) are a guide for the eye. Plots in (b,c) compiled from 7678 traces with no selection. Density map (d) obtained from 1767 traces, selected from a data set of 5036 traces using an automated algorithm, described in Section 2.2 of the SI.

bond, like folding a piece of paper (Figure 1c). $\pi-\pi$ interactions between the two phenyl rings in the syn conformer would then contribute significantly to charge transport (in a way akin to π-stacking), allowing us to detect the interconversion by measuring the junction conductance. This would represent a novel exploitation of mechanically triggered stereoelectronic effects to impart a binary (ON−OFF) conductance switching behavior, incorporating the advantages of π-stacking molecular junctions[12−14] into a single-molecule device.

We therefore synthesized **1** and used the scanning tunneling microscope−break junction technique (STM-BJ)[1] to fabricate its molecular junctions and measure their conductance. In this method, Au point contacts having conductance $G = G_0 \cong 77.48\ \mu S$ are repeatedly fabricated and ruptured by driving an atomically sharp Au wire into and out of contact with a Au on mica substrate. When the process is performed in a solution of a suitable molecular wire, molecular junctions self-assemble in the freshly ruptured point contact, and charge transport can be determined as a function of electrode separation. The process is repeated thousands of times under DC bias voltage V, while recording the current I as a function of the electrode displacement z. Conductance is calculated as $G = I/V$ and the obtained G_z traces are compiled into 1D histograms and 2D density maps yielding, respectively, the distribution of conductance values and the correlation of junction conductance and junction size.

We performed the process in a 1 mM mesitylene solution of **1**, and the results can be observed in Figure 2. The conductance histogram (Figure 2b) shows two main contributions: a high-conductance ($\sim 10^{-3}$ G_0) feature at smaller junction size (~0.8 nm, accounting for the electrodes snapback[19]) and a low conductance feature ($\sim 10^{-4.3}$ G_0) at larger junction size (~1.2 nm including snapback). The results therefore suggest the presence of two possible conformers of **1** in the junction that differ in conductance by more than 1 order of magnitude and in size by 0.4 nm. We then performed piezo-modulation experiments on the fabricated junctions. In these experiments, nanogaps able to accommodate the extended anti conformation (1.2 nm) are initially fabricated, and their size is then modulated by applying a square wave signal to the piezo voltage. The molecule is therefore allowed to assemble in the gap in its thermodynamically favored anti state, and it is then mechanically folded into the syn conformation by compressing the junction. More information on the piezo-modulation experiments can be found in our previous publications on the subject[20,21] and details are provided in the SI. Under a modulation amplitude of 0.4 nm the junctions could be cycled reliably from the high-G to the low-G conformation with excellent repeatability and a conductance increase upon compression by a factor of ~21 (Figure 2d, and more details in the SI).

We can rule out any contributions from variations in the molecule−electrode interface as a mechanism for the observed switching phenomena, as we have already demonstrated that thioanisole contacts do not change binding configuration upon junction compression.[21] Similarly, we can discount an interpretation of our results based on the formation of shorter junctions through Au-carbonyl contacts, as no interactions between a (di)ketone and gold electrodes (e.g., in measurements of molecular wires containing fluorenones,[33] anthraquinones,[34] or diketopyrrolopyrroles[35]) have been reported. To verify that a syn ⇌ anti conformation change is responsible for the observed mechanoresistive effects, we performed power spectral density (PSD) analysis[36] on the junctions in their

https://dx.doi.org/10.1021/acs.nanolett.0c02815
Nano Lett. 2020, 20, 7980−7986

relaxed and compressed state. PSD has been used in the literature to characterize through-space coupling in molecular junctions where charge transport does not follow the chemical bond organization but travels through eigenchannels opened by nonbonding interactions between the molecule and the electrodes,[13,14] between pairs of π-stacking molecules,[14,37] or between different fragments of the same molecule[38] or biomolecule,[39] through intramolecular interactions. When charge transport is purely through-bond, the noise power (the integral of the power spectral density) scales approximately with G, while the scaling increases when charge transport has a through-space character to approach the value found for pure through-space tunneling of G^2. When noise power is normalized by the average conductance G_{AVG} (noise power/G_{AVG}), it is therefore generally found to be insensitive to the junction conductance for through-bond coupling. On the other hand, a strong correlation between noise power/G_{AVG} and G_{AVG} is observed when through-space coupling significantly contributes to charge transport.[36] In order to estimate noise power/G_{AVG}, we performed modulation experiments by fabricating junctions in their relaxed state, recording the current for 50 ms, then compressing them by 0.4 nm and recording the current for another 50 ms (Figure 3a). Slices of

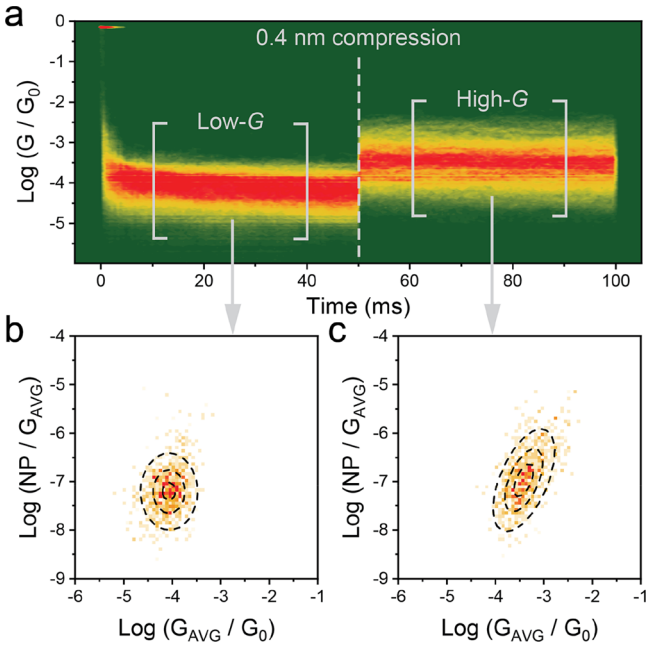

Figure 3. PSD analysis of **1**. (a) Conductance versus time density map for a single compression cycle of **1**. The portions between brackets were then cut off and analyzed with a FFT algorithm to calculate the noise power. (b) Normalized noise power versus G_{AVG} heatmap for **1** in the relaxed, low-G state. (c) Normalized noise power versus G_{AVG} heatmap for **1** in the compressed, high-G state The dashed lines in panels (b,c) are the 25, 50 and 75% height contours of a 2D Gaussian surface fitted to the experimental data. All experiments performed at 200 mV tip−substrate bias. Plots compiled from 8213 traces, using the data selection algorithms described in the SI.

data (30 ms) in the relaxed and stretched state are then analyzed with a fast Fourier transform (FFT) algorithm to obtain the PSD, which is numerically integrated between 100 Hz and 1 kHz to yield the noise power in the region of interest. Normalization by the calculated average conductance of the junction yields noise power/G_{AVG} which is plotted versus G_{AVG} to examine their correlation. More information about the data collection and analysis process can be found in the SI.

Junctions in their relaxed, low-G state showed noise power insensitive to conductance, thus confirming a dominant through-bond mechanism of charge transport (Figure 3b). In the compressed, high-G state, however, noise power strongly correlates with the average conductance of the junction (Figure 3c), indicating that through-space tunneling phenomena are now contributing to the overall charge transport. This further reinforces our proposed interpretation of a mechanoresistive behavior arising from conformational change, where a nonbonding transport channel is opened upon folding the junction to the syn conformation. As a control experiment, we studied the functionalized (*E*)-stilbene **2** ((*E*)-1,2-bis(4-(methylthio)phenyl)ethene, see Figure 4a for structure and

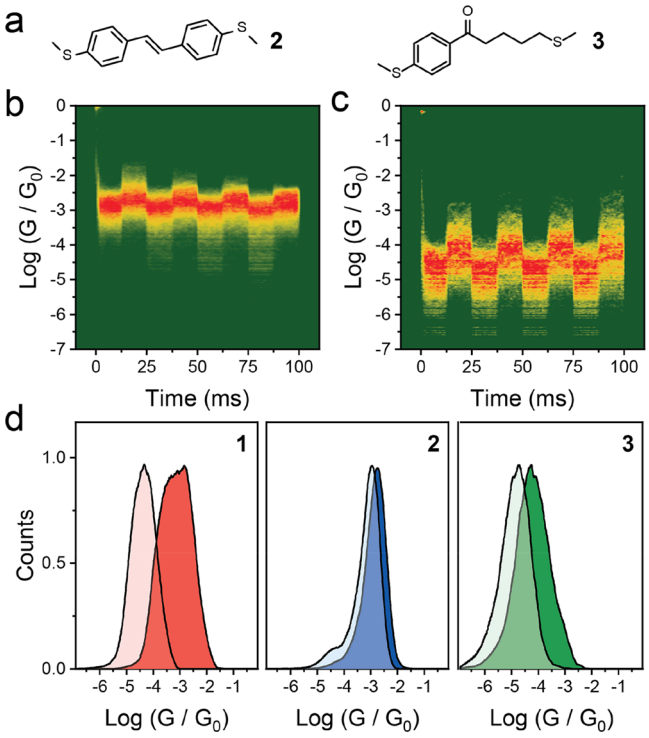

Figure 4. Control experiments. (a) Structures of compounds **2** and **3**. (b) Density map of piezo-modulation experiments for **2**. (c) Density map of piezo-modulation experiments for **3**. (d) Comparison of line profile histograms obtained during modulation experiments (56 and 68 ms). Extended, low conductance junction in shaded, lighter color. Compressed, high-conductance junction in darker, solid color. The conductance boost upon compression is ~21× for **1**, ~2× for **2**, and ~3× for **3**. The same piezo ramp used for compound **1** and shown in Figure 2d was used to obtain the data in (b,c).

the SI for synthetic procedures), which is an analogue of **1** with a central, conformationally locked C═C bond. We found no evidence of mechanically-controlled conductance switching in the STM-BJ and piezo-modulation experiments (see Figure 4b; more details can be found in the SI), showing that (i) a conformationally flexible molecule is needed to attain the switching behavior and (ii) direct electrode−electrode tunneling does not contribute significantly to the overall charge transport with the piezo ramps used in this study. Furthermore, PSD analysis (see SI) indicates a purely through-bond charge transport mechanism (i.e., noise power/G_{AVG} insensitive to G_{AVG}) in both the relaxed and compressed state

https://dx.doi.org/10.1021/acs.nanolett.0c02815
Nano Lett. 2020, 20, 7980−7986

of junctions fabricated with the rigid **2**. Our results may also provide a novel explanation for high-conductance features at short junction extensions, which have been seen in similar foldable molecules incorporating two phenyl rings such as MeS−C_6H_4−Q−Q−Q−C_6H_4−SMe (Q = CH_2, $SiMe_2$, $GeMe_2$).[40,41] It is worth noting that the prominence of the high conductance feature is significantly greater in our data compared to these systems, where it only appears as a weak peak in the histograms. We attribute this increased prominence to the sp^2 hybridization of the diketone bridge of **1** (in contrast with the −Q−Q−Q− sp^3 hybridization) that results in a preferential rotation around the (O═C)—(C═O) axis and a more efficient folding of the junction to the high-conductance state, which is also energetically favored by the relatively long C—C bond (1.54 Å in the solid-state crystal structure of **1**). To provide further confirmation of the proposed mechanism, we also synthesized compound **3**, that features only one phenyl ring and a carbonyl group (5-(methylthio)-1-(4-(methylthio)-phenyl)pentan-1-one, see Figure 4a for structure and the SI for synthetic procedures). The absence of a phenyl ring means that no $\pi-\pi$ interactions are present upon junction compression, and in fact only a small, three-fold mechanically controlled conductance switching was observed, demonstrating the need for two interacting π-systems to attain high conductance in the compressed state (Figure 4d shows a comparison of the three systems investigated). Furthermore, analysis of the conductance signal in the domain of frequency demonstrated that an intermediate through-bond/through-space mechanism of charge transport is operative for **3** in both the relaxed and compressed junction states, in contrast to the clear transition observed in **1** (see SI for further details on the control experiments).

We then performed density functional theory (DFT) quantum transport calculations on the junction in the relaxed and extended states, by imposing constraints on the distance between the two metallic electrodes and letting the molecular portion of the junction relax to its energy minimum. DFT modeling predicts a total energy difference between the anti and the syn conformation of 0.38 eV and a dihedral torsional barrier of 0.42 eV (40.5 kJ/mol, in good agreement with the MM2 Force Field calculations; further details in the SI). Key here is that the conformation interconversion energy barrier is less than the binding energy between the molecule and the Au electrodes (0.54 eV), and we therefore expect the molecule to fold around the conformationally flexible C—C bond as the junction is compressed. Our calculations show that the molecule is therefore likely to adopt a syn conformation upon junction compression (Figure 5a). The Gollum code[42] was then used to calculate the transmission coefficient $T(E)$ for electrons of energy E passing from the source to the drain electrode of the junction, through molecule **1**. The electrical conductance then was obtained using the Landauer formula, and we analyzed the whole behavior of $T(E)$ within the HOMO−LUMO gap (see section 4 of the SI). Transport calculations on the two states (Figure 5b) show that the value of $T(E)$ is indeed strongly dependent on molecular conformation. Our calculations show that $T(E)$ is lower for the anti conformation compared to that of the syn conformation (calculated by constraining the junction size to ~0.8 nm) for the whole energy range between the HOMO and the LUMO, in good qualitative agreement with the experiment. The best quantitative agreement is obtained for energies in the range showed in the gray-shaded region of Figure 5b,

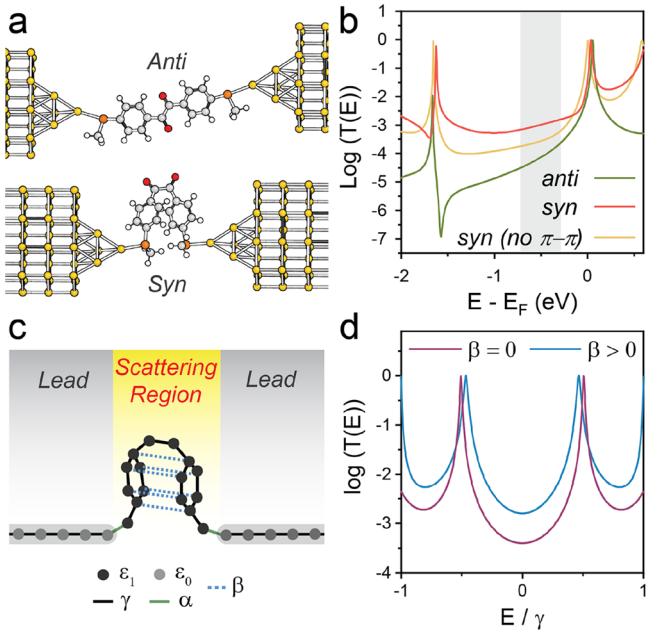

Figure 5. Theoretical calculations. (a) Structure of the junctions obtained by DFT and used for the transport calculations. (b) $T(E)$ curves for compound **1** in the relaxed (anti) and compressed (syn) junction conformations, with and without through-space ($\pi-\pi$) couplings. The gray-shaded area represents the range of energy values where there is good agreement with the experimental data. (c) Schematic depiction of the junction structure used in the tight-binding calculations. (d) Tight-binding transmission function for **1** in the syn configuration, with $\epsilon_0 = \epsilon_1 = 0$, $\gamma = -1$, and $\alpha = -0.2$.

where $T(E)$ increases by more than 1 order of magnitude in the compressed syn conformation.

The change of the (C═O)—(C═O) dihedral angle leads to a rotation of the two phenyl rings toward a face-to-face orientation. In addition, the force applied to the two halves of the molecule (when the electrode−electrode distance is reduced) moves them toward each other to form a new electronic coupling between the π-orbitals of the two phenyl rings (i.e., a stereoelectronic effect). This $\pi-\pi$ interaction opens a new transport channel through the molecule that allows efficient short-range through-space tunneling, responsible for the observed boost in molecular conductance. To verify the proposed mechanism, we set the through-space couplings in the DFT Hamiltonian of the syn conformation (Hamiltonian matrix elements between orbitals of the two halves of the molecule) to zero, and recalculated $T(E)$. We found that $T(E)$ of the syn conformation with through-space couplings is significantly higher than that of the syn conformation without through-space couplings, and only in the former is there a satisfactory agreement with the experimental results where conductance increased by more than 1 order of magnitude upon junction compression (Figure 5b). This is further demonstrated by a single-orbital-per-atom tight-binding model (Figure 5c). Here, a scattering region (the molecule, black) is weakly coupled to two one-dimensional leads (gray). We then calculated $T(E)$ in the absence and presence of through-space couplings β (dotted blue lines). We found that transmission through this simple model increases only when $\beta \neq 0$, which is in agreement with our DFT calculations and the experimental results (Figure 5d).

https://dx.doi.org/10.1021/acs.nanolett.0c02815
Nano Lett. 2020, 20, 7980−7986

In conclusion, we present here a novel way to impart mechanosensitivity to molecular junctions, by exploiting a flexible diketone moiety. We found a large increase in conductance upon compression of the junction, and power spectral density analysis combined with density functional theory calculations demonstrated that mechanosensitivity arises from an anti ⇌ syn conformation switch, as the molecule is folded along the flexible bond following junction compression. Intramolecular nonbonding interactions are increased in the folded syn state, allowing through-space charge tunneling that "shortcuts" a poorly conductive fragment of the molecule. The effect is completely decoupled from the metallic electrodes, and it arises from the formation of a new transport channel through $\pi-\pi$ (stacking) interactions. The switching is reversible and robust, and fabricated junctions can be reliably cycled between high and low conductance states. Our results show the promise, beyond simple electronic decoupling,[43] of deliberately introducing flexible fragments in otherwise rigid molecular wires and the fine degree of control on molecular conformation (and hence, charge transport properties) that can be attained in single-molecule junctions. Furthermore, they highlight the possibility of characterizing intramolecular charge transport phenomena using power spectral density analysis.

METHODS

Chemicals. Compound **1** was synthesized by treating 2 equiv of 4-bromothioanisole with equimolar *n*-butyllithum, followed by transmetalation to copper (as LiBr adduct), and quenching with 1 equiv of oxalyl chloride, following the protocol for the preparation of α-diones developed by Babudri et al.[44] Compound **2** was synthesized by Wittig olefination of 4-(methylthio)benzaldehyde with 4-(methylthio)-benzyltriphenylphosphonium bromide, adapting a literature procedure.[45] Compound **3** was synthesized by reaction of 4-(methylthio)benzoyl chloride with (4-methylthio)butyl)magnesium chloride. Detailed experimental procedure and characterization data can be found in the SI.

STM-BJ Measurements. Junctions were fabricated and characterized using the STM-BJ technique,[1] using a modified Keysight 5500 STM. Further details on the equipment used, the data acquisition process, and its analysis are available in our previous publications on the subject[20,21] and a summary is presented in the SI.

DFT and Transport Calculations. The optimized geometry with ground-state Hamiltonian and overlap matrix elements were obtained using DFT and the SIESTA[46] code. These results were then combined with the Gollum[42] implementation of the nonequilibrium Green's function method[47] to calculate the phase-coherent, elastic-scattering properties of the system, consisting of two gold electrodes and the molecule as the scattering region. Further details are available in the SI.

ASSOCIATED CONTENT

Supporting Information

The Supporting Information is available free of charge at https://pubs.acs.org/doi/10.1021/acs.nanolett.0c02815.

Synthetic procedures and characterization; additional details on STM-BJ measurements; control experiments; additional details on DFT calculations (PDF)

AUTHOR INFORMATION

Corresponding Authors

Andrea Vezzoli − *Department of Chemistry and Stephenson Institute for Renewable Energy, University of Liverpool, Liverpool L69 7ZD, United Kingdom;* orcid.org/0000-0002-8059-0113; Email: andrea.vezzoli@liverpool.ac.uk

Hatef Sadeghi − *School of Engineering, University of Warwick, Coventry CV4 7AL, United Kingdom;* orcid.org/0000-0001-5398-8620; Email: hatef.sadeghi@warwick.ac.uk

Authors

Chuanli Wu − *Department of Chemistry, University of Liverpool, Liverpool L69 7ZD, United Kingdom; School of Chemistry and Materials Science, Nanjing Normal University, Nanjing 210023, People's Republic of China*

Demetris Bates − *Department of Chemistry, University of Liverpool, Liverpool L69 7ZD, United Kingdom*

Sara Sangtarash − *School of Engineering, University of Warwick, Coventry CV4 7AL, United Kingdom*

Nicoló Ferri − *Department of Chemistry, University of Liverpool, Liverpool L69 7ZD, United Kingdom*

Aidan Thomas − *Department of Chemistry, University of Liverpool, Liverpool L69 7ZD, United Kingdom*

Simon J. Higgins − *Department of Chemistry, University of Liverpool, Liverpool L69 7ZD, United Kingdom;* orcid.org/0000-0003-3518-9061

Craig M. Robertson − *Department of Chemistry, University of Liverpool, Liverpool L69 7ZD, United Kingdom;* orcid.org/0000-0002-4789-7607

Richard J. Nichols − *Department of Chemistry, University of Liverpool, Liverpool L69 7ZD, United Kingdom;* orcid.org/0000-0002-1446-8275

Complete contact information is available at: https://pubs.acs.org/10.1021/acs.nanolett.0c02815

Author Contributions

⊥C.W., D.B., S.S. contributed equally to this work.

Notes

The authors declare no competing financial interest.

Raw single-molecule conductance data acquired for this study and the software used for its analysis are available free of charge on the Research Data Catalogue of the University of Liverpool at the address http://datacat.liverpool.ac.uk/id/eprint/1038 and at DOI: 10.17638/datacat.liverpool.ac.uk/1038

ACKNOWLEDGMENTS

We thank Prof. Donald Bethell for useful discussion. C.W. acknowledges funding from the China Scholarship Council (Grant 201806860023). A.V. acknowledges funding from the Royal Society (University Research Fellowship URF \R1\191241) and the School of Physical Sciences of the University of Liverpool (start-up funds and Early Career Researchers grant). S.S. thanks the Leverhulme Trust for funding (Early Career Fellowship ECF-2018-375). H.S. thanks UKRI for funding (Future Leaders Fellowship MR/S015329/2). R.J.N., A.V., and S.J.H. are grateful for financial assistance from the EPSRC (Grants EP/M029522/1 and EP/M005046/1).

REFERENCES

(1) Xu, B.; Tao, N. Measurement of Single-Molecule Resistance by Repeated Formation of Molecular Junctions. *Science* **2003**, *301* (5637), 1221−1223.

(2) Haiss, W.; Nichols, R. J.; van Zalinge, H.; Higgins, S. J.; Bethell, D.; Schiffrin, D. J. Measurement of Single Molecule Conductivity Using the Spontaneous Formation of Molecular Wires. *Phys. Chem. Chem. Phys.* **2004**, *6*, 4330−4337.

(3) Vezzoli, A.; Brooke, R. J.; Higgins, S. J.; Schwarzacher, W.; Nichols, R. J. Single-Molecule Photocurrent at a Metal−Molecule−Semiconductor Junction. *Nano Lett.* **2017**, *17* (11), 6702−6707.

(4) Venkataraman, L.; Klare, J. E.; Tam, I. W.; Nuckolls, C.; Hybertsen, M. S.; Steigerwald, M. L. Single-Molecule Circuits with Well-Defined Molecular Conductance. *Nano Lett.* **2006**, *6* (3), 458−462.

(5) Zhou, J.; Chen, G.; Xu, B. Probing the Molecule-Electrode Interface of Single-Molecule Junctions by Controllable Mechanical Modulations. *J. Phys. Chem. C* **2010**, *114* (18), 8587−8592.

(6) Arroyo, C. R.; Leary, E.; Castellanos-Gómez, A.; Rubio-Bollinger, G.; González, M. T.; Agraït, N. Influence of Binding Groups on Molecular Junction Formation. *J. Am. Chem. Soc.* **2011**, *133* (36), 14313−14319.

(7) Li, C.; Pobelov, I.; Wandlowski, T.; Bagrets, A.; Arnold, A.; Evers, F. Charge Transport in Single Au | Alkanedithiol | Au Junctions: Coordination Geometries and Conformational Degrees of Freedom. *J. Am. Chem. Soc.* **2008**, *130* (1), 318−326.

(8) Haiss, W.; van Zalinge, H.; Bethell, D.; Ulstrup, J.; Schiffrin, D. J.; Nichols, R. J. Thermal Gating of the Single Molecule Conductance of Alkanedithiols. *Faraday Discuss.* **2006**, *131*, 253−264.

(9) Franco, I.; George, C. B.; Solomon, G. C.; Schatz, G. C.; Ratner, M. A. Mechanically Activated Molecular Switch through Single-Molecule Pulling. *J. Am. Chem. Soc.* **2011**, *133* (7), 2242−2249.

(10) Schneebeli, S. T.; Kamenetska, M.; Cheng, Z.; Skouta, R.; Friesner, R. A.; Venkataraman, L.; Breslow, R. Single-Molecule Conductance through Multiple π-π-Stacked Benzene Rings Determined with Direct Electrode-to-Benzene Ring Connections. *J. Am. Chem. Soc.* **2011**, *133* (7), 2136−2139.

(11) Bai, M.; Liang, J.; Xie, L.; Sanvito, S.; Mao, B.; Hou, S. Efficient Conducting Channels Formed by the π-π Stacking in Single [2,2]Paracyclophane Molecules. *J. Chem. Phys.* **2012**, *136* (10), 104701.

(12) Frisenda, R.; Janssen, V. A. E. C.; Grozema, F. C.; van der Zant, H. S. J.; Renaud, N. Mechanically Controlled Quantum Interference in Individual π-Stacked Dimers. *Nat. Chem.* **2016**, *8* (12), 1099−1104.

(13) Li, X.; Wu, Q.; Bai, J.; Hou, S.; Jiang, W.; Tang, C.; Song, H.; Huang, X.; Zheng, J.; Yang, Y.; et al. Structure-Independent Conductance of Thiophene-Based Single-Stacking Junctions. *Angew. Chem., Int. Ed.* **2020**, *59* (8), 3280−3286.

(14) Fu, T.; Smith, S.; Camarasa-Gómez, M.; Yu, X.; Xue, J.; Nuckolls, C.; Evers, F.; Venkataraman, L.; Wei, S. Enhanced Coupling Through π-Stacking in Imidazole-Based Molecular Junctions. *Chem. Sci.* **2019**, *10* (43), 9998−10002.

(15) Ghane, T.; Nozaki, D.; Dianat, A.; Vladyka, A.; Gutierrez, R.; Chinta, J. P.; Yitzchaik, S.; Calame, M.; Cuniberti, G. Interplay between Mechanical and Electronic Degrees of Freedom in π-Stacked Molecular Junctions: From Single Molecules to Mesoscopic Nanoparticle Networks. *J. Phys. Chem. C* **2015**, *119* (11), 6344−6355.

(16) Wu, S.; González, M. T.; Huber, R.; Grunder, S.; Mayor, M.; Schönenberger, C.; Calame, M. Molecular Junctions Based on Aromatic Coupling. *Nat. Nanotechnol.* **2008**, *3* (9), 569−574.

(17) Martín, S.; Grace, I.; Bryce, M. R.; Wang, C.; Jitchati, R.; Batsanov, A. S.; Higgins, S. J.; Lambert, C. J.; Nichols, R. J. Identifying Diversity in Nanoscale Electrical Break Junctions. *J. Am. Chem. Soc.* **2010**, *132* (26), 9157−9164.

(18) Chen, L.; Wang, Y.-H.; He, B.; Nie, H.; Hu, R.; Huang, F.; Qin, A.; Zhou, X.-S.; Zhao, Z.; Tang, B. Z. Multichannel Conductance of Folded Single-Molecule Wires Aided by Through-Space Conjugation. *Angew. Chem., Int. Ed.* **2015**, *54* (14), 4231−4235.

(19) Quek, S. Y.; Kamenetska, M.; Steigerwald, M. L.; Choi, H. J.; Louie, S. G.; Hybertsen, M. S.; Neaton, J. B.; Venkataraman, L. Mechanically Controlled Binary Conductance Switching of a Single-Molecule Junction. *Nat. Nanotechnol.* **2009**, *4* (4), 230−234.

(20) Ismael, A. K.; Wang, K.; Vezzoli, A.; Al-Khaykanee, M. K.; Gallagher, H. E.; Grace, I. M.; Lambert, C. J.; Xu, B.; Nichols, R. J.; Higgins, S. J. Side-Group-Mediated Mechanical Conductance Switching in Molecular Junctions. *Angew. Chem., Int. Ed.* **2017**, *56* (48), 15378−15382.

(21) Ferri, N.; Algethami, N.; Vezzoli, A.; Sangtarash, S.; McLaughlin, M.; Sadeghi, H.; Lambert, C. J.; Nichols, R. J.; Higgins, S. J. Hemilabile Ligands as Mechanosensitive Electrode Contacts for Molecular Electronics. *Angew. Chem., Int. Ed.* **2019**, *58* (46), 16583−16589.

(22) Taniguchi, M.; Tsutsui, M.; Yokota, K.; Kawai, T. Mechanically-Controllable Single Molecule Switch Based on Configuration Specific Electrical Conductivity of Metal-Molecule-Metal Junctions. *Chem. Sci.* **2010**, *1* (2), 247−253.

(23) Kiguchi, M.; Ohto, T.; Fujii, S.; Sugiyasu, K.; Nakajima, S.; Takeuchi, M.; Nakamura, H. Single Molecular Resistive Switch Obtained via Sliding Multiple Anchoring Points and Varying Effective Wire Length. *J. Am. Chem. Soc.* **2014**, *136* (20), 7327−7332.

(24) Meisner, J. S.; Kamenetska, M.; Krikorian, M.; Steigerwald, M. L.; Venkataraman, L.; Nuckolls, C. A Single-Molecule Potentiometer. *Nano Lett.* **2011**, *11* (4), 1575−1579.

(25) Bruot, C.; Hihath, J.; Tao, N. Mechanically Controlled Molecular Orbital Alignment in Single Molecule Junctions. *Nat. Nanotechnol.* **2012**, *7* (1), 35−40.

(26) Jia, C.; Guo, X. Molecule−Electrode Interfaces in Molecular Electronic Devices. *Chem. Soc. Rev.* **2013**, *42* (13), 5642.

(27) Su, T. a.; Li, H.; Steigerwald, M. L.; Venkataraman, L.; Nuckolls, C. Stereoelectronic Switching in Single-Molecule Junctions. *Nat. Chem.* **2015**, *7* (3), 215−220.

(28) Xin, N.; Wang, J.; Jia, C.; Liu, Z. Z. Z.; Zhang, X.; Yu, C.; Li, M.; Wang, S.; Gong, Y.; Sun, H.; et al. Stereoelectronic Effect-Induced Conductance Switching in Aromatic Chain Single-Molecule Junctions. *Nano Lett.* **2017**, *17* (2), 856−861.

(29) Stefani, D.; Weiland, K. J.; Skripnik, M.; Hsu, C.; Perrin, M. L.; Mayor, M.; Pauly, F.; van der Zant, H. S. J. Large Conductance Variations in a Mechanosensitive Single-Molecule Junction. *Nano Lett.* **2018**, *18* (9), 5981−5988.

(30) Brown, C. J.; Sadanaga, R. The Crystal Structure of Benzil. *Acta Crystallogr.* **1965**, *18* (2), 158−164.

(31) Lopes, S.; Gómez-Zavaglia, A.; Lapinski, L.; Chattopadhyay, N.; Fausto, R. Matrix-Isolation FTIR Spectroscopy of Benzil: Probing the Flexibility of the C-C Torsional Coordinate. *J. Phys. Chem. A* **2004**, *108* (40), 8256−8263.

(32) Pawelka, Z.; Koll, A.; Zeegers-Huyskens, T. Solvent Effect on the Conformation of Benzil. *J. Mol. Struct.* **2001**, *597* (1−3), 57−66.

(33) Alanazy, A.; Leary, E.; Kobatake, T.; Sangtarash, S.; González, M. T.; Jiang, H.-W.; Bollinger, G. R.; Agräit, N.; Sadeghi, H.; Grace, I.; et al. Cross-Conjugation Increases the Conductance of Meta-Connected Fluorenones. *Nanoscale* **2019**, *11* (29), 13720−13724.

(34) Hong, W.; Valkenier, H.; Mészáros, G.; Manrique, D. Z.; Mishchenko, A.; Putz, A.; García, P. M.; Lambert, C. J.; Hummelen, J. C.; Wandlowski, T. An MCBJ Case Study: The Influence of π-Conjugation on the Single-Molecule Conductance at a Solid/Liquid Interface. *Beilstein J. Nanotechnol.* **2011**, *2*, 699−713.

(35) Zhang, Y.-P.; Chen, L.; Zhang, Z.-Q.; Cao, J.; Tang, C.; Liu, J.; Duan, L.-L.; Huo, Y.; Shao, X.; Hong, W.; et al. Distinguishing Diketopyrrolopyrrole Isomers in Single-Molecule Junctions via Reversible Stimuli-Responsive Quantum Interference. *J. Am. Chem. Soc.* **2018**, *140* (21), 6531−6535.

(36) Adak, O.; Rosenthal, E.; Meisner, J.; Andrade, E. F.; Pasupathy, A. N.; Nuckolls, C.; Hybertsen, M. S.; Venkataraman, L. Flicker Noise as a Probe of Electronic Interaction at Metal−Single Molecule Interfaces. *Nano Lett.* **2015**, *15* (6), 4143−4149.

https://dx.doi.org/10.1021/acs.nanolett.0c02815
Nano Lett. 2020, 20, 7980−7986

(37) Magyarkuti, A.; Adak, O.; Halbritter, A.; Venkataraman, L. Electronic and Mechanical Characteristics of Stacked Dimer Molecular Junctions. *Nanoscale* **2018**, *10* (7), 3362−3368.
(38) Chen, H.; Zheng, H.; Hu, C.; Cai, K.; Jiao, Y.; Zhang, L.; Jiang, F.; Roy, I.; Qiu, Y.; Shen, D.; et al. Giant Conductance Enhancement of Intramolecular Circuits through Interchannel Gating. *Matter* **2020**, *2* (2), 378−389.
(39) Zhuang, X.; Zhang, A.; Qiu, S.; Tang, C.; Zhao, S.; Li, H.; Zhang, Y.; Wang, Y.; Wang, B.; Fang, B.; et al. Coenzyme Coupling Boosts Charge Transport through Single Bioactive Enzyme Junctions. *iScience* **2020**, *23* (4), 101001.
(40) Su, T. A.; Li, H.; Klausen, R. S.; Widawsky, J. R.; Batra, A.; Steigerwald, M. L.; Venkataraman, L.; Nuckolls, C. Tuning Conductance in $\pi-\sigma-\pi$ Single-Molecule Wires. *J. Am. Chem. Soc.* **2016**, *138* (24), 7791−7795.
(41) Klausen, R. S.; Widawsky, J. R.; Steigerwald, M. L.; Venkataraman, L.; Nuckolls, C. Conductive Molecular Silicon. *J. Am. Chem. Soc.* **2012**, *134* (10), 4541−4544.
(42) Ferrer, J.; Lambert, C. J.; García-Suárez, V. M.; Manrique, D. Z.; Visontai, D.; Oroszlany, L.; Rodríguez-Ferradás, R.; Grace, I.; Bailey, S. W. D.; Gillemot, K.; et al. GOLLUM: A next-Generation Simulation Tool for Electron, Thermal and Spin Transport. *New J. Phys.* **2014**, *16* (9), 093029.
(43) Jia, C.; Migliore, A.; Xin, N.; Huang, S.; Wang, J.; Yang, Q.; Wang, S.; Chen, H.; Wang, D.; Feng, B.; et al. Covalently Bonded Single-Molecule Junctions with Stable and Reversible Photoswitched Conductivity. *Science* **2016**, *352* (6292), 1443−1445.
(44) Babudri, F.; Fiandanese, V.; Marchese, G.; Punzi, A. A Direct Access to α-Diones from Oxalyl Chloride. *Tetrahedron Lett.* **1995**, *36* (40), 7305−7308.
(45) Aradhya, S. V.; Meisner, J. S.; Krikorian, M.; Ahn, S.; Parameswaran, R.; Steigerwald, M. L.; Nuckolls, C.; Venkataraman, L. Dissecting Contact Mechanics from Quantum Interference in Single-Molecule Junctions of Stilbene Derivatives. *Nano Lett.* **2012**, *12* (3), 1643−1647.
(46) Soler, J. M.; Artacho, E.; Gale, J. D.; García, A.; Junquera, J.; Ordejón, P.; Sánchez-Portal, D. The SIESTA Method for Ab Initio Order- N Materials Simulation. *J. Phys.: Condens. Matter* **2002**, *14* (11), 2745−2779.
(47) Sadeghi, H. Theory of Electron, Phonon and Spin Transport in Nanoscale Quantum Devices. *Nanotechnology* **2018**, *29* (37), 373001.

https://dx.doi.org/10.1021/acs.nanolett.0c02815
Nano Lett. 2020, 20, 7980−7986